A UNITED STATES
DEPARTMENT OF
COMMERCE
PUBLICATION

NOAA Technical Memorandum NWS TDL-42

U.S. DEPARTMENT OF COMMERCE
National Oceanic and Atmospheric Administration
National Weather Service

Some Experiments With A Fine-Mesh 500-Millibar Barotropic Model

ROBERT J. BERMOWITZ

Systems
Development
Office

SILVER SPRING, MD.

August 1971

NOAA TECHNICAL MEMORANDA

National Weather Service, Techniques Development Laboratory Series

The primary purpose of the Techniques Development Laboratory of the Office of Systems Development is to translate increases of basic knowledge in meteorology and allied disciplines into improved operating techniques and procedures. To achieve this goal, the Laboratory conducts and sponsors applied research and development aimed at the improvement of diagnostic and prognostic methods for producing weather information. The Laboratory performs studies both for the general improvement of prediction methodology used in the National Meteorological Service System and for the more effective utilization of weather forecasts by the ultimate user.

NOAA Technical Memoranda in the National Weather Service Techniques Development Laboratory series facilitate rapid distribution of material which may be preliminary in nature and which may be published formally elsewhere at a later date. Publications 1 to 5 are in the former series, Weather Bureau Technical Notes (TD), Techniques Development Laboratory (TDL) Reports; publications 6 to 36 are in the former series, ESSA Technical Memoranda, Weather Bureau Technical Memoranda (WBTM). Beginning with TDL 37, publications are now part of the series NOAA Technical Memoranda, National Weather Service (NWS).

Publications listed below are available from the National Technical Information Service, U.S. Department of Commerce, Sills Bldg., 5285 Port Royal Road, Springfield, Va. 22151. Price: $3.00 paper copy; $0.95 microfiche. Order by accession number shown in parentheses at end of each entry.

ESSA Technical Memorandum

WBTM TDL 6 A Fortran Program for the Calculation of Hourly Values of Astronomical Tide and Time and Height of High and Low Water. N. A. Pore and R. A. Cummings, January 1967. (PB-174 660)

WBTM TDL 7 Numerical Experiments Leading to the Design of Optimum Global Meteorological Networks. M. A. Alaka and F. Lewis, February 1967. (PB-174 497)

WBTM TDL 8 An Experiment in the Use of the Balance Equation in the Tropics. M. A. Alaka, D. T. Rubsam, and G. E. Fisher, March 1967. (PB-174 501)

WBTM TDL 9 A Survey of Studies of Aerological Network Requirements. M. A. Alaka, May 1967. (PB-174 984)

WBTM TDL 10 Objective Determination of Sea Level Pressure from Upper Level Heights. William Klein, Frank Lewis, and John Stackpole, May 1967. (PB-179 949)

WBTM TDL 11 Short Range, Subsynoptic Surface Weather Prediction. H. R. Glahn and D. A. Lowry, July 1967. (PB-175 772)

WBTM TDL 12 Charts Giving Station Precipitation in the Plateau States from 700-Mb. Lows During Winter. D. L. Jorgensen, A. F. Korte, and J. A. Bunce, Jr., October 1967. (PB-176 742)

WBTM TDL 13 Interim Report on Sea and Swell Forecasting. N. A. Pore and W. S. Richardson, December 1967. (PB-177 038)

WBTM TDL 14 Meteorological Analysis of 1964-65 ICAO Turbulence Data. DeVer Colson, September 1968. (PB-180 268)

WBTM TDL 15 Prediction of Temperature and Dew Point by Three-Dimensional Trajectories. Ronald M. Reap, September 1968. (PB-180 727)

WBTM TDL 16 Objective Visibility Forecasting Techniques Based on Surface and Tower Observations. Donald M. Gales, October 1968. (PB-180 479)

WBTM TDL 17 Second Interim Report on Sea and Swell Forecasting. N. A. Pore and Lt. W. S. Richardson, USESSA, January 1969. (PB-182 273)

WBTM TDL 18 Conditional Probabilities of Precipitation Amounts in the Conterminous United States. Donald L. Jorgensen, William H. Klein, and Charles F. Roberts, March 1969. (PB-183 144)

WBTM TDL 19 An Operationally Oriented Small-Scale 500-Millibar Height Analysis. Harry R. Glahn and George W. Hollenbaugh, March 1969. (PB-184 111)

WBTM TDL 20 A Comparison of Two Methods of Reducing Truncation Error. Robert J. Bermowitz, May 1969. (PB-184 741)

(Continued inside back cover)

U.S. DEPARTMENT OF COMMERCE
National Oceanic and Atmospheric Administration
National Weather Service

NOAA Technical Memorandum NWS TDL-42

SOME EXPERIMENTS WITH A FINE-MESH 500-MILLIBAR BAROTROPIC MODEL

Robert J. Bermowitz

Systems Development Office
Techniques Development Laboratory

SILVER SPRING, MD.
August 1971

UDC 551.509.313:551.509.324:551.509.334

551.5	Meteorology
.509	Weather forecasts
.313	Numerical prediction
.324	Precipitation forecasts
.334	Circulation forecasts

CONTENTS

SOME EXPERIMENTS WITH A FINE-MESH 500-MILLIBAR BAROTROPIC MODEL

Robert J. Bermowitz

ABSTRACT. The quality and accuracy of 500-mb barotropic predictions that use a fine grid (one-half that used in hemispheric models at the National Meteorological Center, or coarse mesh) in the analysis and forecast are compared to predictions which use the coarse mesh. In addition, fine-mesh, 500-mb predicted heights are used in the Subsynoptic Advection Model (SAM), and the accuracy of the resulting categorical precipitation forecasts compared to those from the operational SAM which uses 500-mb forecasts from the Primitive Equation Model.

Statistical verification of 14 cases shows: (1) a slight decrease in accuracy of predicted 500-mb heights when the fine mesh is used in either the 500-mb forecast, or in both the 500-mb analysis and forecast, and (2) improvement of categorical forecasts of precipitation in the summer season but not in the winter season when fine-mesh, 500-mb heights, predicted from an initial state analyzed on the fine grid, are used in SAM.

INTRODUCTION

Recent efforts to improve the accuracy of numerical forecasts have concentrated on the prediction of events on the subsynoptic scale for periods up to 24 hr. The Subsynoptic Advection Model (SAM) developed within the Techniques Development Laboratory (TDL) and described by Glahn et al. (1969b) is an example of such an effort.

SAM is currently run operationally twice per day at the National Meteorological Center (NMC) on a spatial grid one-fourth that used in hemispheric models at NMC. This model appears to produce forecasts which are superior in sea-level pressure and of about equal quality in categorical precipitation when compared to other machine-produced forecasts. At least part of the success of this model is due to higher resolution initial moisture and sea-level pressure fields (Glahn et al. 1969a) and the relative maintenance of this resolution over the forecast time interval of 17 hr.

It should be noted that SAM is not truly subsynoptic. The gridpoint data needed at the upper level of this model (500-mb heights) are obtained from the synoptic scale NMC Primitive Equation (PE) model (Shuman and Hovermale 1968) and interpolated to the finer SAM grid. Furthermore, the 500-mb heights are time-smoothed (Glahn 1970) to filter gravity waves. As one phase of the continuing developmental effort on SAM, a program was undertaken to determine if finer mesh, 500-mb height input to SAM would produce more accuracy in the precipitation portion of the forecast. Of course, this assumes that use of the finer spatial grid produces better 500-mb height forecasts for periods up to 24 hr.

There are several possible advantages in reducing the mesh length on the 500-mb analysis and forecast grids. For one, more detailed analysis of observational data may be obtained if the density of the upper air network permits. This seems to have been demonstrated by Glahn and Hollenbaugh (1969) in their analysis of 500-mb heights over a portion of the relatively data-dense North American Continent. They employed a gridlength one-half that used in the NMC operational 500-mb analysis. Additionally, smaller scale features in the analyses are more likely to be retained over the forecast interval with the finer spatial grid. However, as Gerrity and McPherson (1969) have indicated, greater resolution of the important physical processes is also a factor in retention of smaller scale features.

Another possible advantage is reduction of the error which results from approximating derivatives by finite differences. This truncation error, which is especially severe in the shorter wave components, results in forecast phase speeds lower than those actually observed. Although truncation error can be reduced by using higher order approximations of the derivative, it seems that, in theory, tolerable error for waves of wavelength less than 2,000 km is possible only by reducing the spatial scale of the grid (Bermowitz 1969).

The studies of Howcroft (1966), Hill (1968), Gerrity and McPherson (1969), Wang and Halpern (1970), and Benwell and Timpson (1968) have demonstrated the advantages of using smaller grids. However, the number of cases investigated was generally small and the comparison between coarse-and fine-mesh models was, for the most part, subjective.

To better determine the practical advantages of using finer spatial grids in both 500-mb height analyses and forecasts, an experiment was performed in which combinations of a coarse mesh (381 km at 60°N) and a fine mesh (one-half coarse gridlength) were used in both analyses and barotropic forecasts. This paper describes the results of these experiments. In addition, it reports on the comparative verification between the categorical precipitation forecasts resulting from the operational SAM, and an experimental SAM which used predicted fine-mesh, 500-mb heights as initial upper level information.

EXPERIMENTAL DESIGN

Precipitation Forecasts

Perhaps the most important aspect of SAM is the precipitation forecast generated by the model. The predicted moisture variable is the saturation deficit S_d defined as

$$S_d = h_5 - S_t$$

where h_5 is the 1000-to 500-mb thickness and S_t is the saturation thickness. If S_t is defined as that 1000-to 500-mb thickness for which precipitation occurs for a given amount of moisture between these levels, then negative values of S_d imply a forecast of precipitation. Conversely, positive values of S_d imply no precipitation.

Since the 500-mb heights used in SAM are, out of necessity, quite smooth, it is possible that increased resolution and accuracy in the predicted heights at this level could improve the forecasts of h_5, and consequently, S_d. (500-mb heights are also used in SAM to forecast the 1000-mb height field.) To test this hypothesis, an experiment was performed in which categorical forecasts of precipitation (yes or no) from the operational SAM (OSAM) were objectively compared to those obtained from an experimental SAM (ESAM). The latter used 500-mb height forecasts obtained from a fine-mesh barotropic prediction model rather than the PE forecasts of 500-mb heights used in OSAM. This was the only difference between ESAM and OSAM.

500-Mb Model

With the possibility of future incorporation of a fine-mesh 500-mb prediction model in OSAM, it was decided that any upper level model to be used in ESAM would have to be relatively simple, yet have the ability to give good forecasts over a 24-hr period. A barotropic model appeared to fit these requirements.

The one that was actually used in the experimental program is a divergent, barotropic model containing a tropopause. A description has been given by Cressman (1958). The prognostic vorticity equation applied at the 500-mb level is

$$\left(\nabla^2 - \frac{\mu\eta}{\Psi}\right)\frac{\partial\Psi}{\partial t} + J(\Psi,\eta) + f\,\vec{\nabla}\cdot\vec{V} = 0, \qquad (1)$$

where the symbols have their customary meteorological or mathematical meanings. Following Cressman (1958), the value of μ was chosen to be 4. In addition, the coefficient of the divergence term was taken to be the Coriolis parameter instead of the absolute vorticity. This was based on the experience with barotropic models reported by Gustafson (1964).

Mountain and friction effects were included in the manner described by Cressman (1960). The divergence at 500-mb, $\vec{\nabla}\cdot\vec{V}$ in (1), is given by

$$\vec{\nabla}\cdot\vec{V} = -\frac{\omega_m + \omega_f}{P_g - 200} ,$$

where ω_m and ω_f are the vertical motions due to mountain and friction effects respectively, and P_g is the height of the terrain in mb. ω_m is expressed as

$$\omega_m = \vec{V}_g \cdot \vec{\nabla} P_g ,$$

where the surface wind $\vec{V}_g$ is approximated from the 500-mb wind $\vec{V}$ in the following manner:

$$\vec{V}_g = \left[1 - 0.8\left(\frac{P_g - 500}{500}\right)\right]\vec{V} .$$

ω_f is related to the components of the surface stress τ_x and τ_y by the equation

$$\omega_f = \frac{g}{f}\left(\frac{\partial \tau_x}{\partial y} - \frac{\partial \tau_y}{\partial x}\right) .$$

The surface stress $\vec{\tau}$ is given by

$$\vec{\tau} = \rho\, C_d \left| \vec{V}_g \right| \vec{V}_g$$

where C_d is the drag coefficient. The utilized terrain and drag coefficient fields were the same as those used in the current NMC PE model, interpolated biquadratically to the fine grid.

Equation (1) was solved in the standard manner on the fine spatial grid within the octagon shown in figure 1. To satisfy the stability criteria, a time step of 20 min was used with the familiar, first forward then centered time difference scheme.

It is probably uneconomical to solve eq (1) over the whole octagon, since the only 500-mb forecast height data that are required as input to SAM are contained in the rectangle bounded by solid lines shown in figure 1. (The rectangle shown by dashed lines indicates the area in which forecasts are produced by SAM.) However, with use of simple boundary conditions (Ψ constant with time) in the solution of eq (1), the whole octagon was used, for experimental purposes, to minimize the effect of any boundary error in the area of interest (solid rectangle).

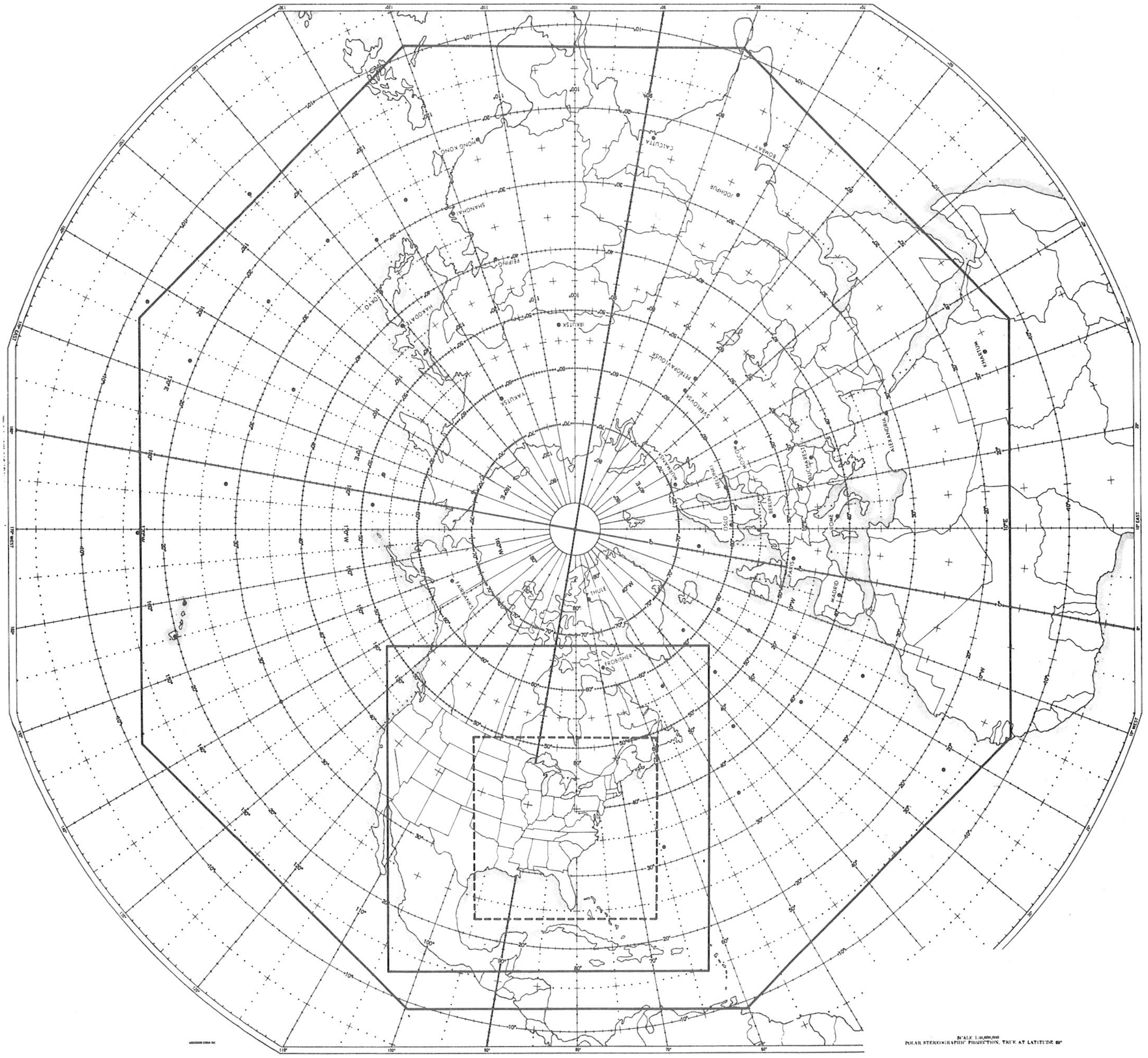

Figure 1.-- Boundaries of the three geographical areas used in the experiments. Hemispheric forecasts of 500-mb heights are made within the octagon. The solid rectangle denotes the area in which fine-mesh, 500-mb height analyses are performed, and the dashed rectangle encloses the SAM grid.

Space derivatives were computed by means of the simple three-point centered difference approximation. The exception to this was the calculation of derivatives that appeared in the Jacobian operator. In this case, a fourth order, five-point approximation was utilized in an attempt to reduce truncation error in excess of that obtainable by using the fine mesh. The finite difference approximation for the x-derivative can be represented schematically as

$$\frac{1}{12d}\left[1 \quad -8 \quad 0 \quad 8 \quad -1\right],$$

where d is the distance between neighboring points.

The stream function Ψ in eq (1) was obtained from the 500-mb height by solving a linearized version of the balance equation which can be written as

$$\nabla^2 \Psi = \frac{g}{f}\left[\nabla^2 z - \frac{1}{f}(\vec{\nabla} f \cdot \vec{\nabla} z)\right]. \qquad (2)$$

Ellsaesser (1968), with use of a barotropic model similar to the one described here, has indicated the suitability of utilizing this particular wind law. The boundary conditions for solution of eq (2) were, very simply, taken to be

$$\Psi = \frac{g}{f_o} z$$

where f_o is the Coriolis parameter at 45°N latitude.

The initial data for the forecasts were the NMC operational 500-mb analyses for the Northern Hemisphere, interpolated biquadratically to the smaller grid. However, a fine-mesh, 500-mb analysis was inserted over the solid rectangular window region in figure 1. A program described by Glahn and Hollenbaugh (1969) was used for this purpose. The two analyses were then merged along their common boundary by means of a nine-point operator described by Shuman (1957). The equation is

$$\bar{z}_{x,y} = z_{x,y} + \frac{1}{2}\alpha(1-\alpha)\,(z_{x-1,y} + z_{x,y+1} + z_{x+1,y} + z_{x,y-1} - 4z_{x,y})$$

$$+ \frac{1}{4}\alpha^2\,(z_{x-1,y+1} + z_{x+1,y+1} + z_{x+1,y-1} + z_{x-1,y-1} - 4z_{x,y}),$$

where $\bar{z}_{x,y}$ is the smoothed 500-mb height at the central point, and α is a smoothing index which was taken to be 0.5. First, the common boundary was smoothed; then these values were used to smooth the rows and columns one gridlength on both sides of the common boundary.

Predicted 500-mb heights are required by SAM on an hourly basis from hours 7 to 24 after upper air observation time. At these times, the forecasted height field from the fine-mesh model was filtered of possible high frequency noise. The smoothed field was not used in subsequent time steps during the solution of eq (1). The smoothing was accomplished at all possible points with a 49-point operator (Gerrity and McPherson 1969) which can be written schematically as

$$\frac{1}{1024}\begin{bmatrix} 1 & 0 & -9 & -16 & -9 & 0 & 1 \\ 0 & 0 & 0 & 0 & 0 & 0 & 0 \\ -9 & 0 & 81 & 144 & 81 & 0 & -9 \\ -16 & 0 & 144 & 256 & 144 & 0 & -16 \\ -9 & 0 & 81 & 144 & 81 & 0 & -9 \\ 0 & 0 & 0 & 0 & 0 & 0 & 0 \\ 1 & 0 & -9 & -16 & -9 & 0 & 1 \end{bmatrix}.$$

Point values that were not smoothed were close enough to the octagonal boundary so that it is unlikely that this would have any adverse effect on the experimental results.

500-Mb Height Forecasts

From a practical point of view, it is not immediately obvious that the fine computational grid introduced in the analysis and barotropic prediction model at 500-mb would be instrumental in producing better forecasts of 500-mb heights for projections up to 24 hr. For example, it is not clear that even the relatively dense upper air observational network over a portion of the North American Continent can justify fine-mesh analyses as initial conditions for a 500-mb barotropic prediction model. That is, do coarse- and fine-mesh analyses differ enough to result in predictions that are significantly different, when each is used as initial conditions in the same forecast model? Also, it is not clear, from a practical viewpoint, that use of the fine computational grid will significantly add to the reduction of truncation error that is obtainable by using a higher order finite difference approximation of the derivative.

In an attempt to gain some information about these problems, another set of experiments was conducted in which the coarse and fine grids were used in various combinations in 500-mb analyses and barotropic forecasts. In all cases, the same 500-mb forecast model, as previously described, was employed. The only difference was the time step, which varied with the gridlength.

One combination has already been discussed in connection with the precipitation forecasts. It is denoted by FMFM for fine-mesh analysis (in the window region) and fine-mesh forecast. Another one combined the NMC operational coarse-mesh analysis interpolated biquadratically to the fine mesh, with a prediction made on the fine grid (CMFM). The only difference between FMFM and CMFM is the insertion of a fine-mesh analysis in the window region.

Thus, a comparison of these forecasts in the window region should shed some light on the utility of fine-mesh analyses as initial conditions for barotropic forecasts.

A third combination used the NMC coarse-mesh analysis with a coarse-mesh forecast (CMCM). Here a time step of 1 hr was used. For subjective comparison only, CMCM predictions were interpolated biquadratically to the fine grid. The only difference between CMFM and CMCM is the gridlength and time step used in the forecast model. Therefore, a comparison of these predictions should provide some practical information about additional reduction of truncation error over that obtainable by using a higher order approximation of the derivative.

RESULTS

500-Mb Height Forecasts

The experiments described above were performed on 14 cases during the period May 1969 to March 1970. The cases were usually selected such that 0000 GMT upper air data and 0700 GMT surface data for Friday were used. In this way, some of the subjectivity was removed from the selection, in addition to which this choice of day coincided with the verification of the operational SAM. For a variety of reasons, it was not always possible to use Friday cases; nevertheless, most of those in the experiment did fall on that day.

Figure 2 shows the coarse-mesh analysis interpolated to the fine grid (dashed) and fine-mesh analysis (solid) for 0000 GMT May 14, 1969. This case is fairly typical of others in the experiment. Note that there is not much difference between the two analyses. In all the cases studied, the largest differences, about 30 m, generally occurred in closed lows. As expected, the shorter waves generally have more definition in the fine-mesh analysis. This is particularly evident west of Washington State, and over northeast British Columbia, the central Rocky Mountain and central Plains States.

Figure 3 illustrates the 24-hr forecasts made from the analyses shown in figure 2. The FMFM forecast is shown in solid, the CMFM in dashed, and the CMCM in dotted lines. It is obvious that the forecasts are not much different, which is not surprising in view of the similarity of the analyses. As expected, detail is retained more by the FMFM and CMFM than by the CMCM.

In order to objectively compare the 500-mb predictions of the several barotropic models, the root mean square error (RMSE) and a gradient skill score (S1) (Teweles and Wobus 1954) were computed for 12- and 24-hr forecasts in the area bounded by the solid rectangle in figure 1. This area contains 1,225 fine-mesh gridpoints. The S1 score is given by

$$S1 = 100 \frac{\sum |E_z|}{\sum |O_z|}$$

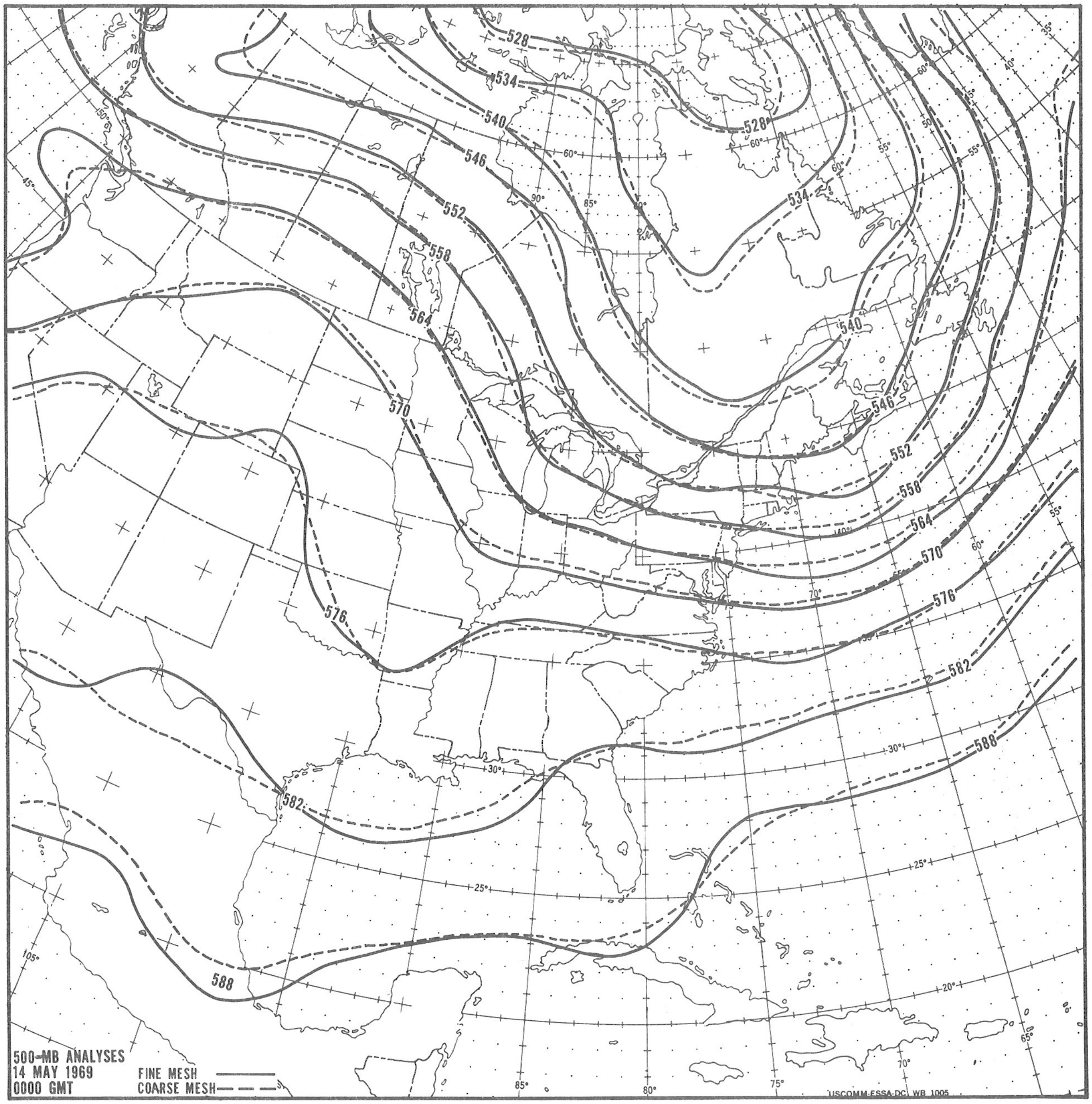

Figure 2.-- Coarse-mesh and fine-mesh 500-mb height analyses for 0000 GMT May 14, 1969. Contours are labeled in decameters.

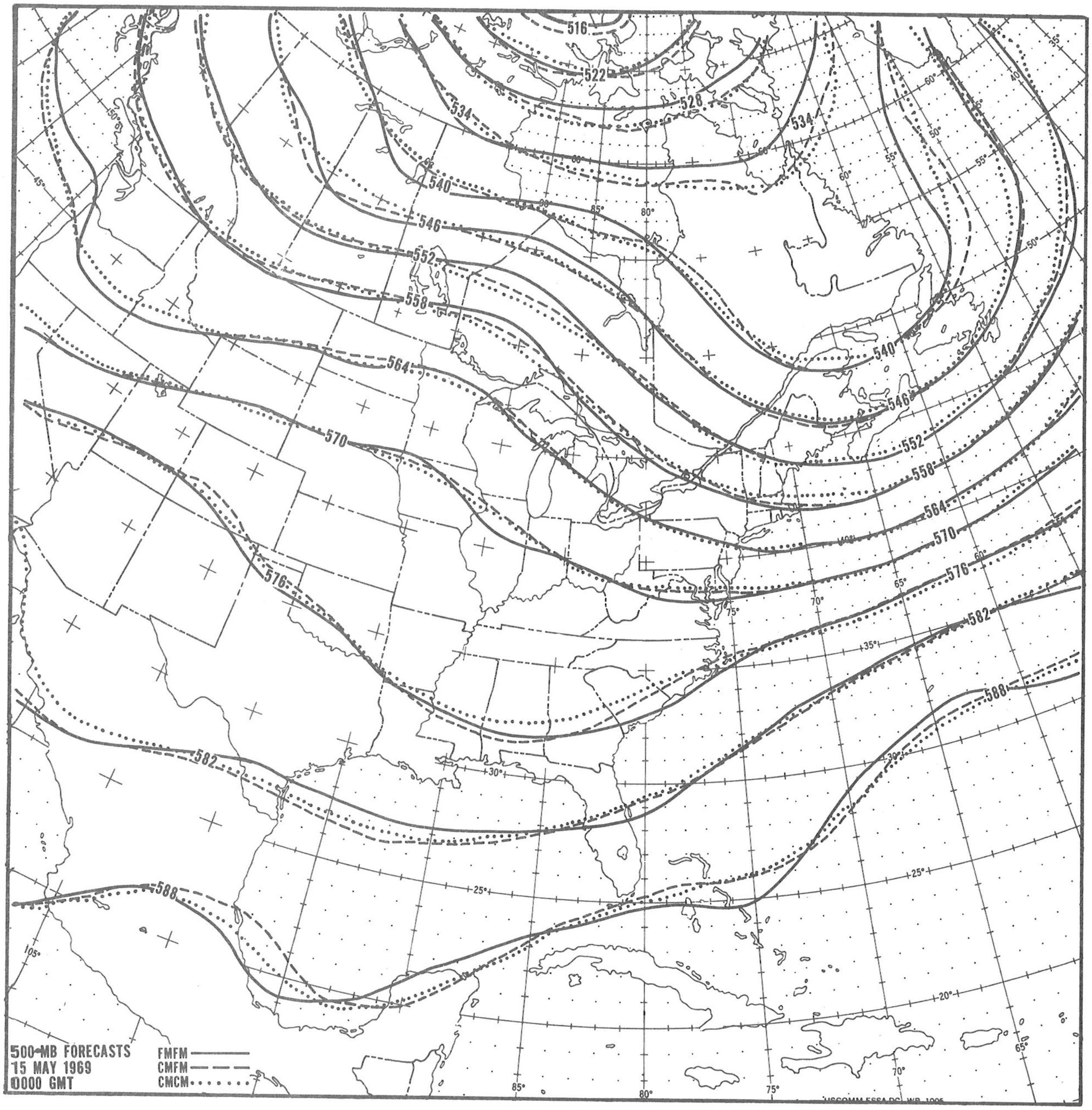

Figure 3.-- 24-hr, 500-mb heights predicted by the barotropic model in which the coarse and fine grids were used in the following three combinations in the analyses and forecasts: fine-mesh analysis/fine-mesh forecast (FMFM), coarse-mesh analysis/fine-mesh forecast (CMFM), coarse-mesh analysis/coarse-mesh forecast (CMCM). Valid time is 0000 GMT May 15, 1969.

where E_z is the error in the forecast height difference between gridpoints, and O_z is the larger of either the observed or forecast height difference between gridpoints. Both the RMSE and S1 score were computed with values at coarse-mesh gridpoints, since it was desirable to avoid interpolated CMCM values in the verification. Although the 14 cases for which the objective comparison was performed is not a large sample, it should be indicative of the relative accuracy of the forecasts.

Table 1 summarizes the RMSE and S1 score for the FMFM, CMFM, CMCM, and PE 12- and 24-hr 500-mb forecasts. The PE forecasts are included for later discussion in connection with the verification of the precipitation forecasts. All forecasts were verified against the NMC operational 500-mb analyses.

Table 1 shows that there is not much difference in the scores of the three barotropic forecasts. It appears that no improvement measurable by these statistical quantities is obtained when the fine mesh is used either in the 500-mb forecast (CMFM) or the 500-mb analysis and forecast (FMFM).

Table 1.--Root mean square error (RMSE) in meters and S1 score of the three barotropic and the PE 12- and 24-hr forecasts. Statistics represent averages of 14 cases.

	RMSE		S1	
	12-HR	24-HR	12-HR	24-HR
FMFM	26.9	43.2	30.5	39.4
CMFM	26.7	44.0	28.2	38.4
CMCM	26.4	43.0	27.8	37.7
PE	23.0	31.4	28.1	35.3

The largest statistical difference among the barotropic forecasts, especially between the FMFM and the others, occurs in the S1 score. Table 1 indicates that the S1 score is related to the detail contained in the barotropic forecasts; the more detailed forecast has the worse S1 score. Therefore, it would seem that either the detail has not been accurately predicted or that the verifying coarse-mesh analysis may be biasing the results in favor of the smoother forecast.

To test the latter, eight cases were also verified against the fine-mesh analysis. Figure 4 shows that when the forecasts are verified against the fine-mesh analysis all the S1 scores worsen, but the difference between these scores for the various models decreases about 45 percent. Thus, while part of the difference among the S1 scores may be due to verification against the coarse-mesh analysis, it appears that the smaller features cannot be predicted with much accuracy by this simple barotropic model.

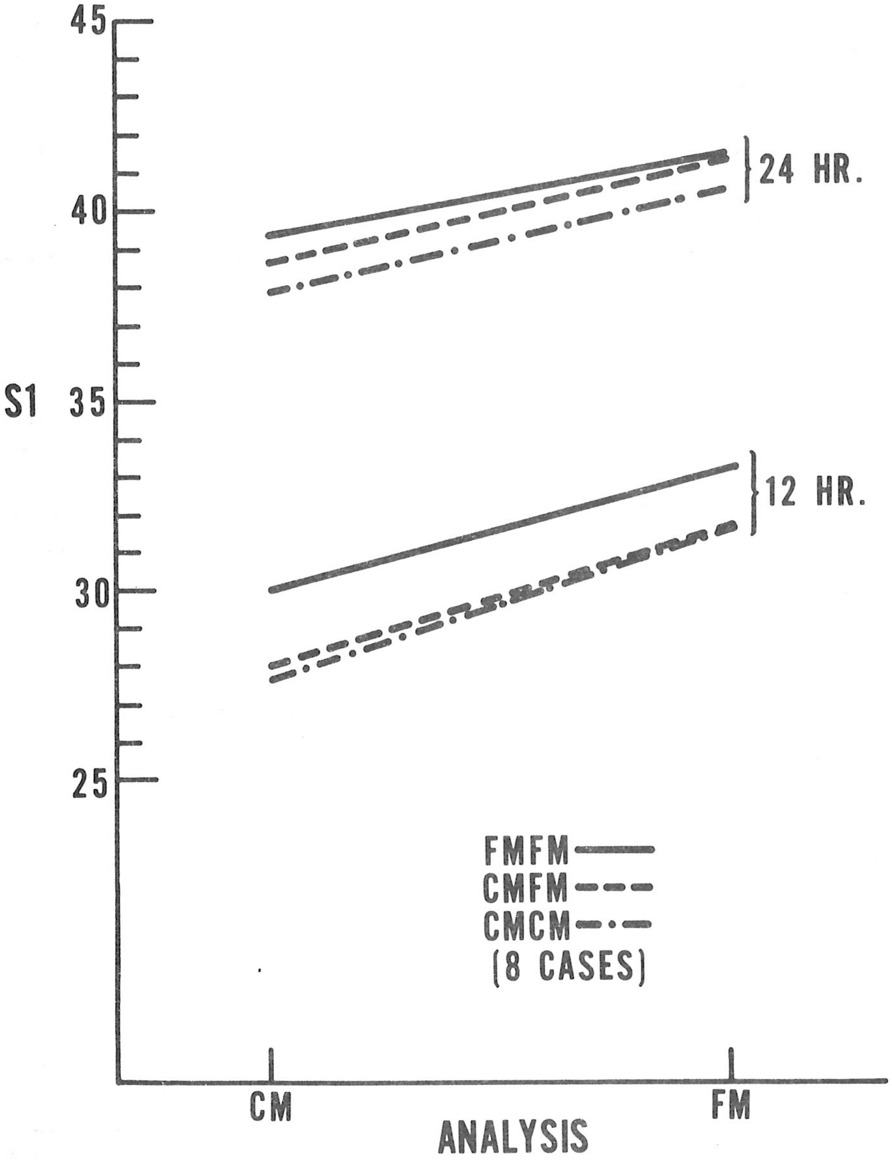

Figure 4.-- The S1 scores of the barotropic forecasts for eight cases as a function of the verifying coarse-and fine-mesh analyses. FMFM, CMFM, and CMCM have the same meanings as in figure 3.

The use of the fine mesh in the forecast added to the reduction of truncation error obtained by utilization of a fourth-order approximation of the derivative. This is illustrated in figure 5, which shows a portion of the 24-hr CMFM and CMCM forecasts valid at 0000 GMT August 10, 1969, and the verifying coarse-mesh analysis. A short wave extending from lower Lake Michigan to north central Missouri (solid) has been predicted closer to this observed position by the CMFM model (dashed) than by the CMCM model (dotted).

Precipitation Forecasts

A comparative verification of categorical precipitation forecasts from OSAM and ESAM, for the 12-hr period 1200 GMT to 2400 GMT, was performed for 21 stations over the eastern half of the United States. An observed occurrence of precipitation was .01 in. during the 12-hr period. A negative value of S_d any time during the period was considered to be a forecast of precipitation. Two observations were missing; thus, the total sample size was 292.

The statistics that were computed for this verification were the same as those which are routinely used in the evaluation of the operational product (Glahn et al. 1969b). They include the threat score of precipitation (T_{sp}), threat score of no precipitation (T_{snp}), post agreement (PA) and prefigurance (PF) which are considered together in a single score by adding them and dividing the sum by 2, and the common (Heidke) skill score (SS). A higher score is desirable for all statistics.

Of the 292 observations, there were 69 observed precipitation cases. OSAM forecast 57 occurrences, thus underforecasting precipitation by approximately 17 percent, while ESAM overforecast by about 25 percent, calling for 86 occurrences. Table 2 indicates that ESAM was approximately 15 percent better than OSAM in T_{sp}, about 12 percent better in (PA + PF)/2, and approximately 18 percent better in SS, while OSAM was about 4 percent better than ESAM in T_{snp}. Considering all the statistics, there was about a 10-percent increase in accuracy in categorical precipitation forecasting by ESAM.

Table 2.-- Threat score of precipitation (T_{sp}), threat score of no precipitation (T_{snp}), Heidke skill score (SS), post agreement (PA) and prefigurance (PF) for 292 categorical precipitation forecasts from the operational (OSAM) and experimental SAM (ESAM) for the 12-hr period, 1200 GMT to 2400 GMT.

	T_{sp}	T_{snp}	SS	(PA + PF)/2
OSAM	.33	.75	.34	.50
ESAM	.38	.72	.40	.56

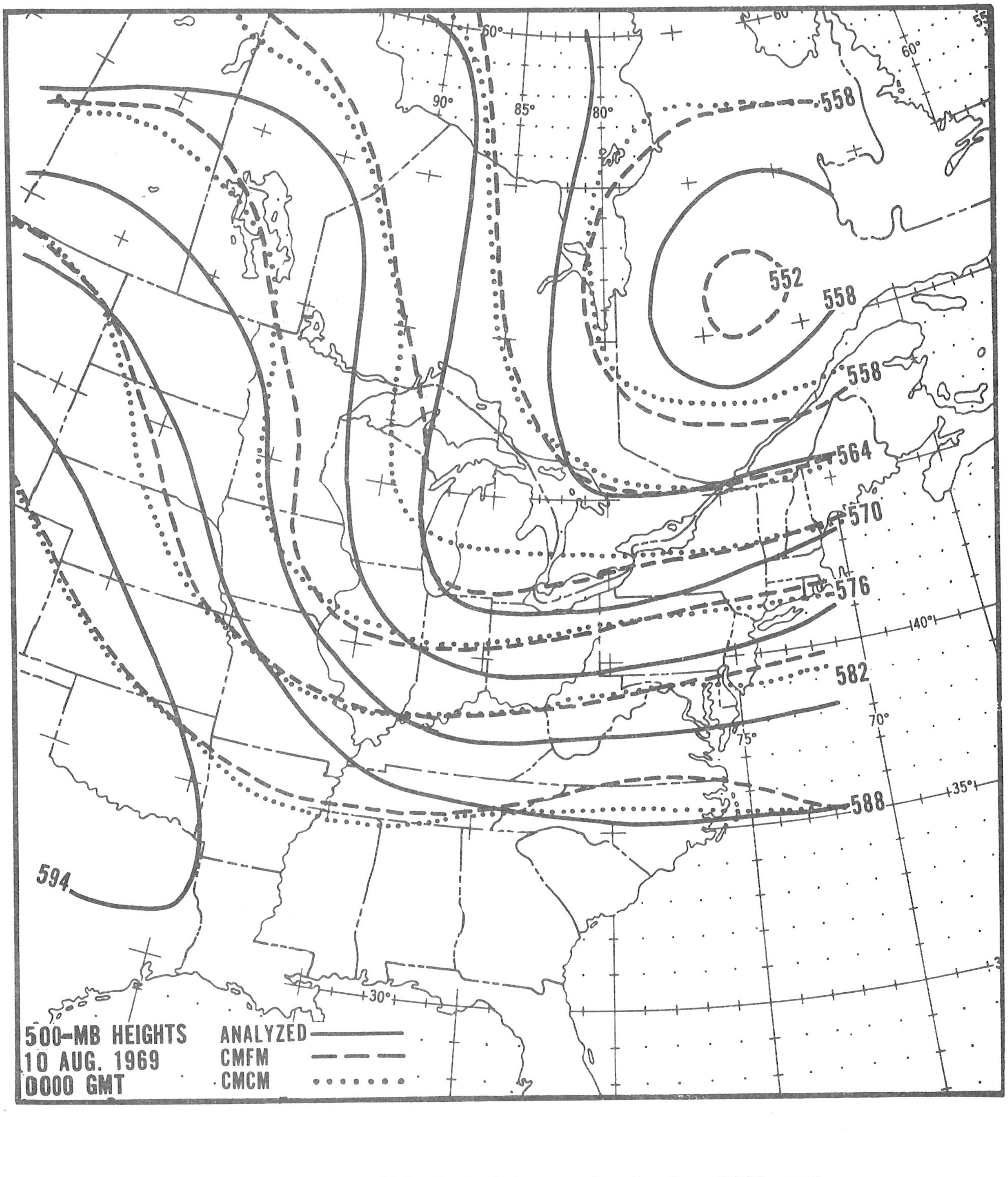

Figure 5.-- Coarse-mesh 500-mb height analysis for 0000 GMT August 10, 1969, and verifying 24-hr coarse-(CMCM) and fine-mesh (CMFM) forecasts. Both forecasts were produced from an initial state analyzed on the coarse mesh.

This improvement is rather contradictory in view of the results presented in table 1, which indicate the superiority of the PE 500-mb forecasts over those from the FMFM. However, analyses of individual cases of improved categorical precipitation forecasts by ESAM indicate that although the overall PE 500-mb forecasts are statistically better in RMSE and S1 score than those from the FMFM, individual 500-mb troughs associated with precipitation can, at times, be more accurately predicted by the FMFM.

An example of this is the case of 14 May, where precipitation was observed at Tallahassee and Jacksonville, Fla. This precipitation was correctly predicted by ESAM but not by OSAM. A comparison of verifying coarse-mesh analyses (solid) with the PE (dotted) and FMFM (dashed) 12- and 24-hr forecasts (figs. 6 and 7), shows that the trough associated with the precipitation, initially extending from western Arkansas southward into the Gulf of Mexico (fig. 2), is more accurately predicted with respect to position and amplitude by the FMFM model than by the PE model.

It is somewhat difficult to ascertain the differences in the precipitation forecasts that would have resulted if the 500-mb heights from the CMCM or CMFM models had been used in SAM instead of those from the FMFM model. No experiments were performed to determine this.

Of some interest, however, is the precipitation at Jacksonville that was correctly predicted by ESAM. As can be seen in figure 3, there is some difference between the predicted heights from the various barotropic forecasts over northern Florida. This difference reaches about 8 m between the FMFM and CMFM models, and about 15 m between the FMFM and CMCM models. Furthermore, an approximate 60-m difference between PE and FMFM 500-mb heights, and an S_d forecast at Jacksonville of 117 m from OSAM and -1 m from ESAM indicate that both CMFM and CMCM 500-mb heights may be too high to result in a forecast of precipitation for Jacksonville. Of course, this is only one example, but it demonstrates the general impression, obtained by analyzing other cases, that the fine mesh introduced into 500-mb height analyses and forecasts can, at times, add useful detail for SAM categorical precipitation prediction.

A seasonal breakdown of the comparative verification of precipitation forecasts produced by ESAM and OSAM is of interest. By definition, the summer season extends from 1 April to 30 September, and the winter season from 1 October to 31 March. Table 3 shows that the overall improvement of ESAM when compared to OSAM is due to the improvement that occurs in the summer season. One possible reason is that relatively weak 500-mb systems, associated with convective type precipitation in the summer season, have less of a tendency to be smoothed with use of the fine mesh than with use of the coarse mesh of the PE model.

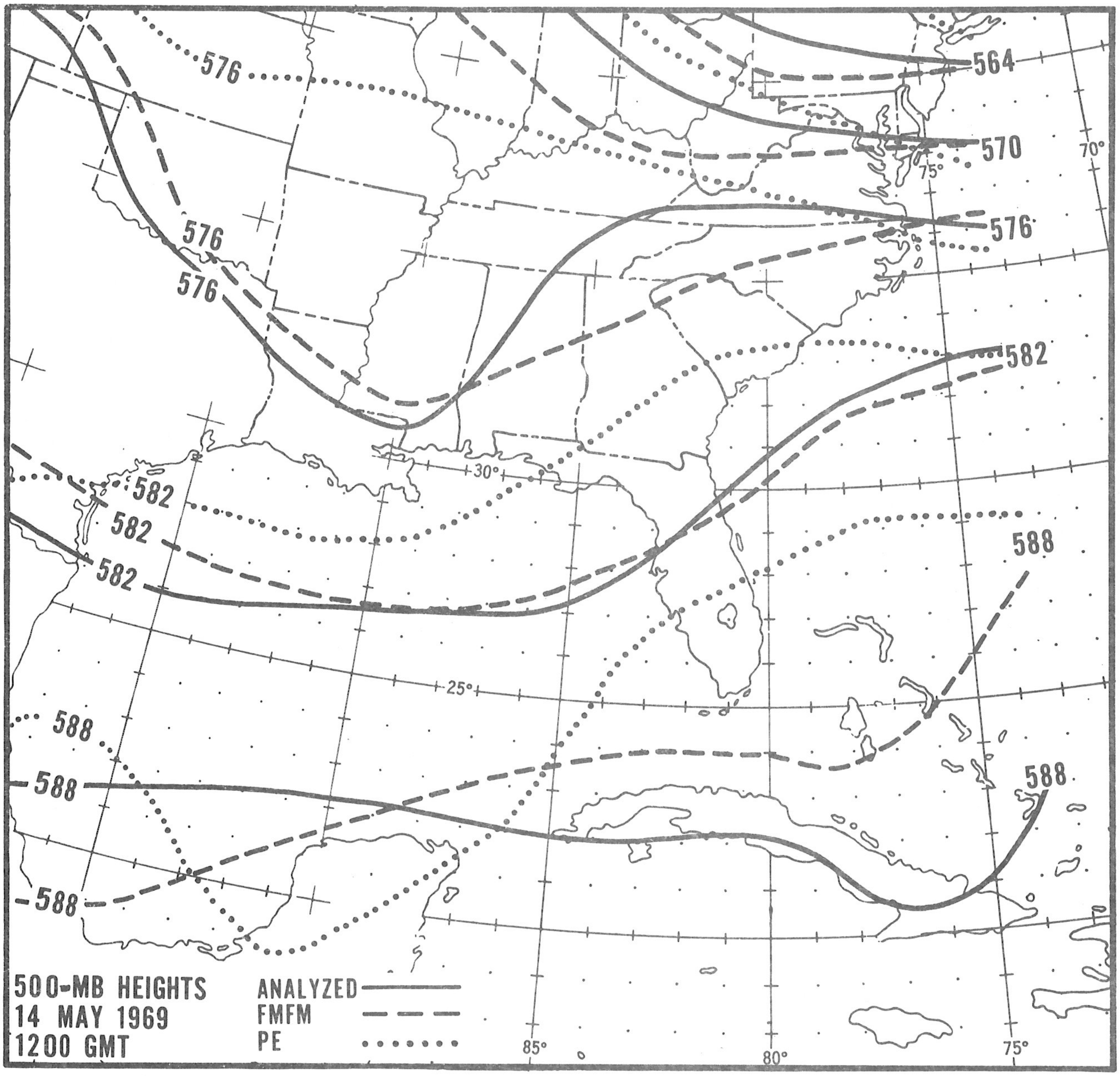

Figure 6.-- Coarse-mesh 500-mb height analysis for 1200 GMT May 14, 1969, and verifying 12-hr Primitive Equation (PE) and fine-mesh (FMFM) forecasts. The fine-mesh forecast was produced from an initial state analyzed on the fine mesh.

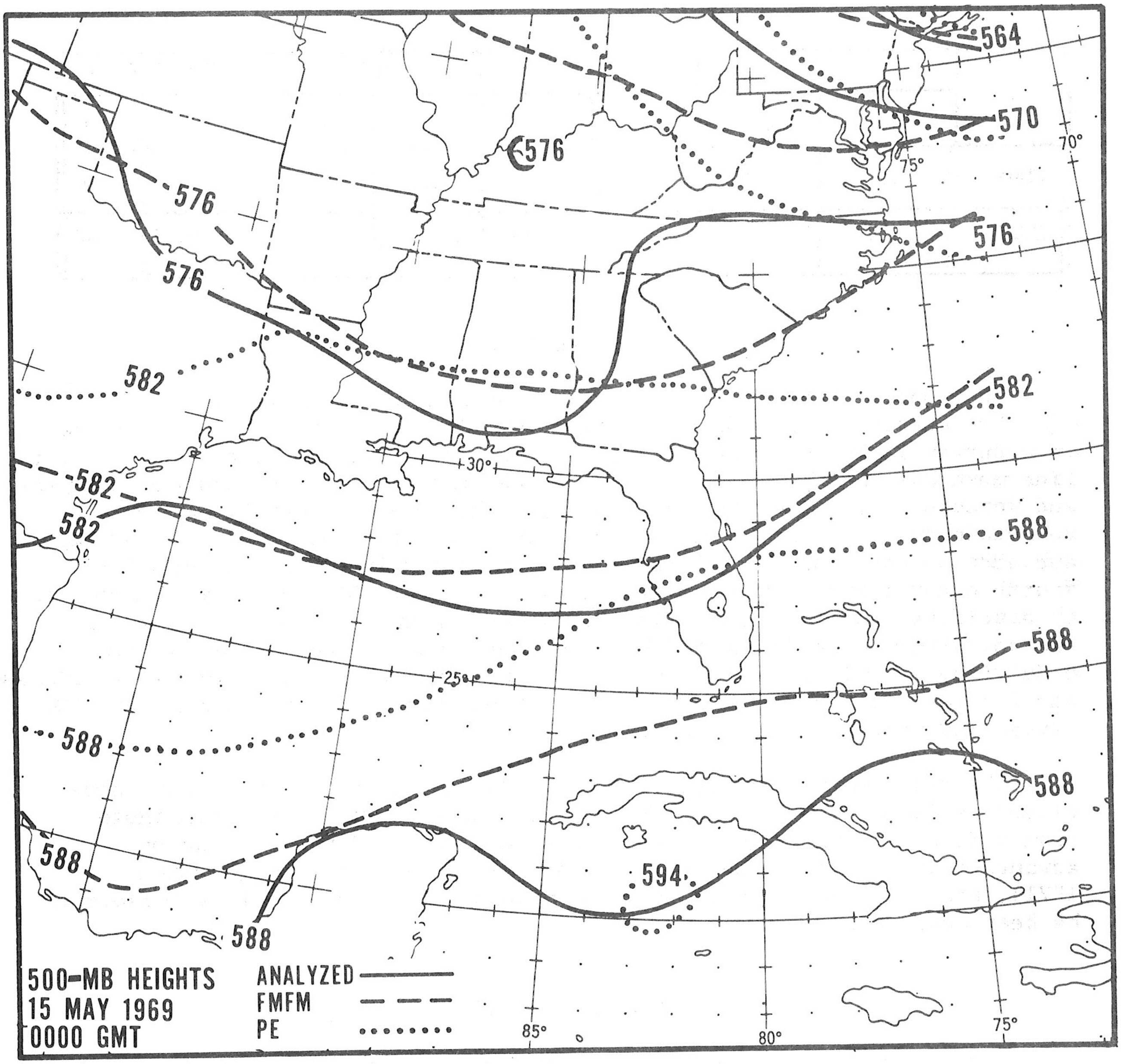

Figure 7.-- Coarse-mesh 500-mb height analysis for 0000 GMT May 15, 1969, and verifying 24-hr Primitive Equation (PE) and fine-mesh (FMFM) forecasts. The fine-mesh forecast was produced from an initial state analyzed on the fine mesh.

Table 3.-- Same verification statistics as in table 2 for 168 summer season (S) and 124 winter season (W) forecasts.

	T_{sp}		T_{snp}		SS		(PA + PF)/2	
	S	W	S	W	S	W	S	W
OSAM	.21	.47	.74	.78	.21	.51	.38	.64
ESAM	.37	.40	.75	.69	.40	.40	.54	.60

CONCLUSIONS

The conclusions from this study can be summarized as follows: (1) Two statistics from a comparative verification show a slight decrease in accuracy in 500-mb height prediction with a barotropic model in which the fine mesh has been introduced in either the forecast, or in both the analysis and forecast. (2) The fine mesh used in the 500-mb forecast model helps to retain smaller scale features over the forecast interval at this level, and adds to the reduction of truncation error obtained through use of a fourth order approximation of the derivative. (3) SAM categorical forecasts of precipitation are improved in the summer season, but not in the winter season, with use of 500-mb heights predicted from a fine-mesh barotropic model from an initial state analyzed on the fine grid. (4) Fine-mesh analyses and forecasts of 500-mb heights can sometimes provide useful detail for SAM categorical precipitation prediction.

The relatively poor performance of ESAM during the winter season precludes replacement of 500-mb heights from the PE model in SAM with those from a fine-mesh barotropic model. However, in the future, it may be advantageous to use 500-mb heights from a fine-mesh PE model (Howcroft 1971), where the positive gains to be made from a reduced spatial scale may be best achieved.

ACKNOWLEDGMENTS

I am indebted to Harry R. Glahn, of the Techniques Development Laboratory, who made numerous helpful suggestions during the course of the study, and provided the prototype 500-mb forecast program upon which the final version was based. In addition, I would like to express my gratitude to George W. Hollenbaugh, also of TDL, for providing and modifying the 500-mb analysis and SAM programs. Finally, I would like to thank the other members of TDL who supported this effort, including Evelyn L. Boston, Dean E. Costantinou, Peter R. Howe, Jackie Hughes, Betty Wells, and Patricia E. Robinson.

REFERENCES

Benwell, G.R.R., and Timpson, M. S., "Further Work with the Bushby-Timpson 10-Level Model," Quarterly Journal of the Royal Meteorological Society, Vol. 94, No. 399, Jan. 1968, pp. 12-24.

Bermowitz, R. J., "A Comparison of Two Methods of Reducing Truncation Error," ESSA Technical Memorandum WBTM TDL-20, May 1969, 7 pp.

Cressman, G. P., "Barotropic Divergence and Very Long Atmospheric Waves," Monthly Weather Review, Vol. 86, No. 8, Aug. 1958, pp. 293-297.

Cressman, G. P., "Improved Terrain Effects in Barotropic Forecasts," Monthly Weather Review, Vol. 88, No. 9-12, Sept.-Dec. 1960, pp. 327-342.

Ellsaesser, H. W., "Comparative Test of Wind Laws for Numerical Weather Prediction," Monthly Weather Review, Vol. 96, No. 5, May 1968, pp. 277-285.

Gerrity, J. P.,Jr., and McPherson, R. D., "Development of a Limited Area Fine-Mesh Prediction Model," Monthly Weather Review, Vol. 97, No. 9, Sept. 1969, pp. 665-669.

Glahn, H. R., and Hollenbaugh, G. W., "An Operationally Oriented Small-Scale 500-Millibar Height Analysis Program," ESSA Technical Memorandum WBTM TDL-19, Mar. 1969, 17 pp.

Glahn, H. R., Hollenbaugh, G. W., and Lowry, D. A., "An Operationally Oriented Objective Analysis Program," ESSA Technical Memorandum WBTM TDL-22, July 1969a, 20 pp.

Glahn, H. R., Lowry, D. A., and Hollenbaugh, G. W., "An Operational Subsynoptic Advection Model," ESSA Technical Memorandum WBTM TDL-23, July 1969b, 26 pp.

Glahn, H. R., "Filtering Gravity Waves from 500-mb Heights Forecast by the PE Model," Operating Location H, Headquarters, Air Weather Service, Suitland, Md. and Techniques Development Laboratory, National Weather Service, NOAA, Silver Spring, Md., Nov. 1970, 13 pp., (unpublished manuscript).

Gustafson, A. F., "Mesh Model 1964," Office Note 24, National Meteorological Center, U.S. Weather Bureau, Suitland, Md., Dec. 1964, 7 pp.

Hill, G. E., "Grid Telescoping in Numerical Weather Prediction," Journal of Applied Meteorology, Vol. 7, No. 2, Feb. 1968, pp. 29-38.

Howcroft, J. G., "Fine-Mesh Limited-Area Forecasting Model," Technical Report 188, Air Weather Service, Scott Air Force Base, Ill., Nov. 1966, pp. 71-75.

Howcroft, J. G., "Local Forecast Model: Present Status and Preliminary Verification," Office Note 50, National Meteorological Center, National Weather Service, Suitland, Md., Jan. 1971, 23 pp.

Shuman, F. G., "Numerical Methods in Weather Prediction: II. Smoothing and Filtering," Monthly Weather Review, Vol. 85, No. 11, Nov. 1957, pp. 357-361.

Shuman, F. G., and Hovermale, J. B., "An Operational Six-Layer Primitive Equation Model," Journal of Applied Meteorology, Vol. 7, No. 4, Aug. 1968, pp. 525-547.

Teweles, S., Jr., and Wobus, H. B., "Verification of Prognostic Charts," Bulletin of the AMS, Vol. 35, No. 10, Dec. 1954, pp. 455-463.

Wang, H. H., and Halpern, P., "Experiments with a Regional Fine-Mesh Prediction Model," Journal of Applied Meteorology, Vol. 9, No. 4, Aug. 1970, pp. 545-553.

(Continued from inside front cover)

WBTM TDL 21 Automatic Decoding of Hourly Weather Reports. George W. Hollenbaugh, Harry R. Glahn, and Dale A. Lowry, July 1969. (PB-185 806)

WBTM TDL 22 An Operationally Oriented Objective Analysis Program. Harry R. Glahn, George W. Hollenbaugh, and Dale A. Lowry, July 1969. (PB-186 129)

WBTM TDL 23 An Operational Subsynoptic Advection Model. Harry R. Glahn, Dale A. Lowry, and George W. Hollenbaugh, July 1969. (PB-186 389)

WBTM TDL 24 A Lake Erie Storm Surge Forecasting Technique. William S. Richardson and N. Arthur Pore, August 1969. (PB-185 778)

WBTM TDL 25 Charts Giving Station Precipitation in the Plateau States From 850- and 500-Millibar Lows During Winter. August F. Korte, Donald L. Jorgensen, and William H. Klein, September 1969. (PB-187 476)

WBTM TDL 26 Computer Forecasts of Maximum and Minimum Surface Temperatures. William H. Klein, Frank Lewis, and George P. Casely, October 1969. (PB-189 105)

WBTM TDL 27 An Operational Method for Objectively Forecasting Probability of Precipitation. Harry R. Glahn and Dale A. Lowry, October 1969. (PB-188 660)

WBTM TDL 28 Techniques for Forecasting Low Water Occurrences at Baltimore and Norfolk. Lt. (jg) James M. McClelland, USESSA, March 1970. (PB-191 744)

WBTM TDL 29 A Method for Predicting Surface Winds. Harry R. Glahn, March 1970. (PB-191 745)

WBTM TDL 30 Summary of Selected Reference Material on the Oceanographic Phenomena of Tides, Storm Surges, Waves, and Breakers. Arthur N. Pore, May 1970. (PB-193 449)

WBTM TDL 31 Persistence of Precipitation at 108 Cities in the Conterminous United States. Donald L. Jorgensen and William H. Klein, May 1970. (PB-193 599)

WBTM TDL 32 Computer-Produced Worded Forecasts. Harry R. Glahn, June 1970. (PB-194 262)

WBTM TDL 33 Calculation of Precipitable Water. L. P. Harrison, June 1970. (PB-193 600)

WBTM TDL 34 An Objective Method for Forecasting Winds Over Lake Erie and Lake Ontario. Celso S. Barrientos, August 1970. (PB-194 586)

WBTM TDL 35 A Probabilistic Prediction in Meteorology: A Bibliography. A. H. Murphy and R. A. Allen, June 1970. (PB-194 415)

WBTM TDL 36 Current High Altitude Observations--Investigation and Possible Improvement. M. A. Alaka and R. C. Elvander, July 1970. (Com-71-00003)

NOAA Technical Memorandum

NWS TDL 37 Prediction of Surface Dew Point Temperatures. R. C. Elvander, January 1971. (Com-71-00253)

NWS TDL 38 Objectively Computed Surface Diagnostic Fields. Robert J. Bermowitz, February 1971. (Com-71-00301)

NWS TDL 39 Computer Prediction of Precipitation Probability for 108 Cities in the United States. William H. Klein, February 1971. (Com-71-00249)

NWS TDL 40 Wave Climatology for the Great Lakes. N. A. Pore, J. M. McClelland, and C. S. Barrientos, February 1971. (Com-71-00368)

NWS TDL 41 Twice-Daily Mean Monthly Heights in the Troposphere Over North America and Vicinity. August F. Korte, June 1971.